Electric field tuning of magnetism in heterostructure of yttrium iron garnet film/lead magnesium niobate-lead zirconate titanate ceramic

Jianyun Lian, Freddy Ponchel, Nicolas Tiercelin, Ying Chen, Denis Remiens, Tuami Lasri, Genshui Wang, Philippe Pernod, Wenbin Zhang, Xianlin Dong

Applied Physics Letters

Electric field tuning of magnetism in heterostructure of yttrium iron garnet film/ lead magnesium niobate-lead zirconate titanate ceramic

Cite as: Appl. Phys. Lett. **112**, 162904 (2018); https://doi.org/10.1063/1.5023885
Submitted: 29 January 2018 • Accepted: 03 April 2018 • Published Online: 17 April 2018

Jianyun Lian, Freddy Ponchel, Nicolas Tiercelin, et al.

Electric field tuning of magnetism in heterostructure of yttrium iron garnet film/lead magnesium niobate-lead zirconate titanate ceramic

Jianyun Lian,[1,2,3] Freddy Ponchel,[2] Nicolas Tiercelin,[2] Ying Chen,[1,3,a)] Denis Rémiens,[2,b)] Tuami Lasri,[2] Genshui Wang,[1] Philippe Pernod,[2] Wenbin Zhang,[1] and Xianlin Dong[1,c)]
[1]*Key Laboratory of Inorganic Functional Materials and Devices, Shanghai Institute of Ceramics, Chinese Academy of Sciences, 1295 Dingxi Road, Shanghai 200050, People's Republic of China*
[2]*Joint International Laboratory LIA LICS, University Lille, CNRS, Centrale Lille, ISEN, University Valenciennes, UMR 8520-IEMN, F-59000 Lille, France*
[3]*University of Chinese Academy of Sciences, 19 A Yuquan Rd., Shijingshan District, Beijing 100049, People's Republic of China*

(Received 29 January 2018; accepted 3 April 2018; published online 17 April 2018)

In this paper, the converse magnetoelectric (CME) effect by electric field tuning of magnetization in an original heterostructure composed of a polycrystalline yttrium iron garnet (YIG) film and a lead magnesium niobate-lead zirconate titanate (PMN-PZT) ceramic is presented. The magnetic performances of the YIG films with different thicknesses under a DC electric field applied to the PMN-PZT ceramics and a bias magnetic field are investigated. All the magnetization-electric field curves are found to be in good agreement with the butterfly like strain curve of the PMN-PZT ceramic. Both the sharp deformation of about 2.5‰ of PMN-PZT and the easy magnetization switching of YIG are proposed to be the reasons for the strongest CME interaction in the composite at the small electric coercive field of PMN-PZT (4.1 kV/cm) and the small magnetic coercive field of YIG (20 Oe) where the magnetic susceptibility reaches its maximum value. A remarkable CME coefficient of 3.1×10^{-7} s/m is obtained in the system with a 600 nm-thick YIG film. This heterostructure combining multiferroics and partially magnetized ferrite concepts is able to operate under a small or even in the absence of an external bias magnetic field and is more compact and power efficient than the traditional magnetoelectric devices. *Published by AIP Publishing.*
https://doi.org/10.1063/1.5023885

The ME composites with an advanced functionality of independent optimization of both ferroic phases and the allowance of room temperature operation have attracted considerable interest for diverse potential applications in ME memory, spintronic, and microwave signal processing devices.[1–5] As a product-property of layered ME composites, the ME effect is defined as the electric field control of magnetism or vice versa and facilitated by interface mechanical deformation arising from the magnetostrictive or inverse piezoelectric effect.[4] In particular, achieving the same degree of magnetic controllability using an electric field is potentially a faster process and involves lower energy consumption.[3,6]

Until now, strain-mediated, voltage-controlled magnetic performances (magnetocrystalline anisotropy, magnetic domains, and magnetoresistance) in ME composites have been widely studied and in particular through the ferromagnetic resonance (FMR) effect.[3–8] Most of the studies tended to choose an Yttrium iron garnet ($Y_3Fe_5O_{12}$, YIG) as the ferromagnetic phase due to its outstanding advantages including small magnetocrystalline anisotropy, narrow ferromagnetic resonance linewidth, high resistivity, and low microwave loss.[9–12] Therefore, many efforts have been devoted to the voltage tuning of FMR on composites of YIG/BST and YIG/PZT. These YIGs were always more than 4 μm thick and mechanically coupled with ferroelectric materials using epoxy which greatly weaken the ME effect.[1,11,12] Most importantly, it is an indirect method to understand the converse magnetoelectric (CME) effect based on the FMR shift. In recent years, special attention has been paid on another piezoelectric material, the PMN-PT in single crystal form, for its extraordinary piezoelectric coefficient ($d_{33} = 1500$ pm/V).[13] However, the related investigations have mainly focused on the voltage tunable FMR effect for microwave device applications. Shastry *et al.* established a model for the microwave CME interaction through FMR in the case of a bilayer of the (111) YIG film-(001) PMN-PT single crystal and observed that the CME coefficient range (2.3–5.4 Oe kV/cm) depends on the YIG film thickness and the magnetic field orientation.[13] An electric field tunable resonator was realized with E = 0–8 kV/cm applied to a similar structure, and a maximum frequency shift of 22 MHz was obtained for the tangential magnetization.[14] A voltage tunable phase shifter on the same structure exhibited a phase shift of 119° under an electric field of 11 kV/cm.[15] The research on strain-modulated, electric field-controlled magnetization, which is actually the most direct manifestation of the CME effect, has not been reported on the composite of YIG/PMN-PZT.

In this work, we use the $0.25Pb(Mg_{1/3}Nb_{2/3})O_3$–$0.75Pb(Zr_{0.48}Ti_{0.52})O_3$ (0.25PMN-0.75PZT) ceramic as the piezoelectric phase to be coupled with the YIG film because the 0.25PMN-0.75PZT ceramic has superior electrical properties than the single-phase PMN and PZT materials since its composition is close to the morphotropic phase boundary (MPB)[16] and the large field-induced strain of 2.2‰ is an important factor to obtain a high CME effect.[17] This work

a)Electronic mail: chenying@mail.sic.ac.cn
b)Electronic mail: denis.remiens@univ-valenciennes.fr
c)Electronic mail: xldong@mail.sic.ac.cn

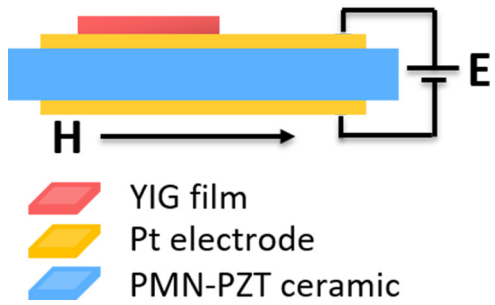

FIG. 1. The schematic of the YIG/Pt/PMN-PZT/Pt heterostructure with the direction of *E* and *H*.

constitutes the direct investigation on the CME effect by voltage tuning of magnetization for this composite structure, and the enhanced CME coefficient is achieved by comprehensive consideration of the electric field, magnetic field, and film thickness.

The schematic describing the YIG/PMN-PZT composite is shown in Fig. 1. The YIG films with three different thicknesses (200, 400, and 600 nm) were grown on 0.5 mm-thick 0.25PMN-0.75PZT metallized ceramics by magnetron sputtering without any gluing between them. Before YIG film deposition, an important step of ceramic polishing was made, and Pt electrodes were deposited on both faces of the ceramics by magnetron sputtering. The ceramic dimension is $8 \times 8\,mm^2$, while Pt electrodes and YIG films are limited to $6 \times 6\,mm^2$ and $5 \times 3\,mm^2$, respectively, by using metallic masks. The Pt electrodes are 100 nm thick.

Each step that leads to the fabrication of the heterostructures (ceramic polishing, deposition, etc.) and their characterizations (structure, microstructure, interface, etc.) has been checked and validated. The sputtering conditions and ceramic fabrication details are given in Refs. 16 and 18. In this letter, we focus only on the electric, magnetic, and magnetoelectric properties of the structure. The electric hysteresis loop (*P-E*) and field-induced strain behavior (*S-E*) of the PMN-PZT ceramic are obtained with a standard ferroelectric tester (TF analyzer 2000, aixACCT, Germany). The magnetic hysteresis loops (*M-H*) are measured at room temperature by using a Vibration Sample Magnetometer (VSM) (ADE model EV9). The voltage tuning of magnetization is performed by combining the VSM with an external high voltage source (0–12 kV) via two coppers attached to the upper and lower electrodes of the sample in a VSM test chamber. Then, it is possible for our homemade system to polarize the sample by applying a high DC voltage to the ceramic and to modify the magnetic state of YIG under a magnetic field simultaneously. The heterostructures with the same initial magnetized state are subjected to an electric field *E* changing as the following cycle: 0 kV/cm, −12 kV/cm, 12 kV/cm, −12 kV/cm, and finally 0 kV/cm across PMN-PZT and different bias in-plane magnetic fields *H* (80, 20, and 10 Oe) along the width of the YIG film.

In theory, the field-induced strain originated from the piezoelectric ceramic can be transferred into the ferrite film, leading to the internal magnetic field variation due to the piezomagnetic effect, which is equivalent to a magnetizing field and controls the ferrite magnetization. Namely, the CME effect to be presented here is based on the fact that magnetization modification is strain dependent and its magnitude is determined by the mechanical deformation.[14] We first focus on the electric hysteresis loop and strain curve of the 0.25PMN-0.75PZT ceramic (without YIG film). As shown in Fig. 2, when an ac electric field of 12 kV/cm with a frequency of 0.01 Hz is applied to the ceramic, there is a sharp strain peak (2.5‰) at its small electric coercive field (4.3 kV/cm), while the 0.72PMN-0.28PT (001) single crystal can only reach a strain of 0.5‰ at its coercive field.[17] Therefore, it is promising to obtain a large magnetization shift with a small electric field using this ceramic. After fabricating the complete heterostructure, the characterization of X-ray diffraction is examined, and the results show that all the YIG films present a good crystallization in the desired phase of cubic $Y_3Fe_5O_{12}$ without any second phase. When the YIG film thickness increases, we observe an enhancement of the peak intensity, indicating a better film crystallization.

The magnetic hysteresis loops of YIG films with the applied in-plane magnetic field along the film width, after removing the effect of Pt/PMN-PZT/Pt and electric contact wires,[19] are shown in Fig. 3(a) and its inset for different thicknesses (*t*). The corresponding saturation magnetization (*Ms*), residual magnetization (*Mr*), and coercive field (H_C) are listed in Table I. It is observed that with the increase in the YIG film thickness, *Ms* increases and *Hc* drops slightly since the thicker film has better crystallinity and less roughness. All *Hc* values, close to 20 Oe, are lower than those of YIG films fabricated on silicon,[18] and $4\pi Ms = 1843$ Gs for the 600 nm-thick YIG is a little higher than the value (1800 Gs) for the epitaxial YIG films on a gadolinium gallium garnet single crystal,[1] denoting that YIG films grown on PMN-PZT ceramics can also exhibit good magnetic properties and good crystallization. The magnetic field dependency of magnetic susceptibility (χ) of YIG films extracted from the first derivative of their *M-H* loops is shown in Fig. 3(b). The maximum values of χ (χ_{max}) for every thickness are listed in Table I. The highest χ_{max} is obtained for the 400 nm-thick YIG film, and a similar value is measured for 600 nm, but for the thinner film of 200 nm, we observe a lower value. It is worth mentioning that all the χ_{max} values are obtained at a magnetic field of 20 Oe which corresponds to *Hc* [Fig. 3(b)]. That is to say, when the magnetic domains of YIG films are

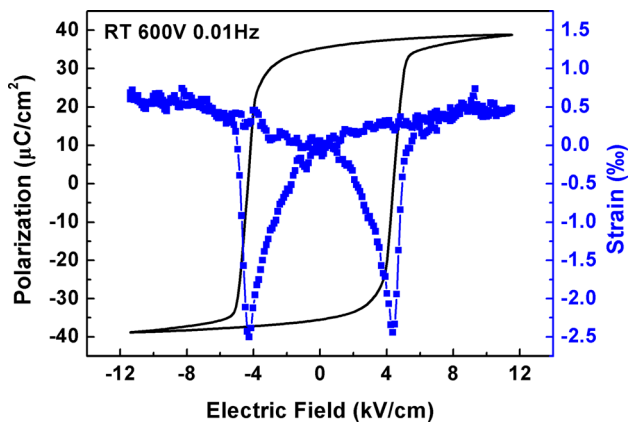

FIG. 2. The electric hysteresis loop and field-induced strain of the 0.25PMN-0.75PZT ceramic, the applied voltage is 600 V, and the frequency is 0.01 Hz.

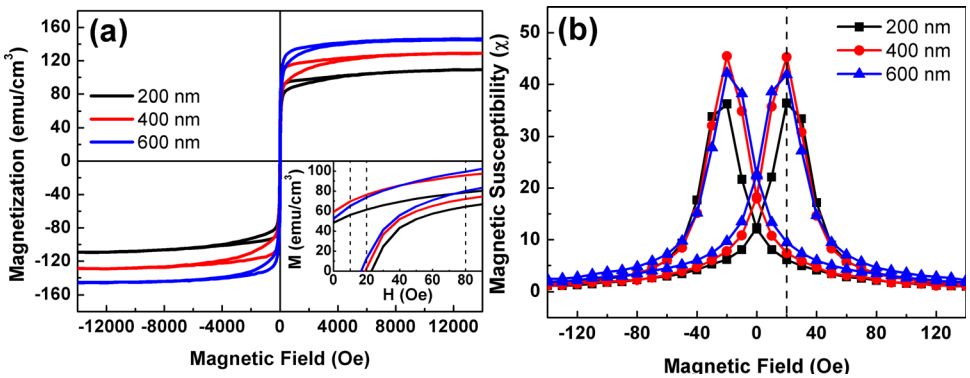

FIG. 3. The magnetic hysteresis loops (a) and enlarged loops [inset of (a)] and the magnetic susceptibility curves (b) of YIG films with different thicknesses excluding the effect of Pt/PMN-PZT/Pt and wires.

completely disordered, they can be arranged easily along the external magnetic field.

In order to understand the CME effect and calculate the CME coefficients for this system, we investigate the influence of the electric field applied to the ceramics on the magnetization in YIG films of different thicknesses under a series of bias magnetic fields (80, 20, and 10 Oe). As an illustration, Fig. 4(a) presents the magnetization as a function of the electric field (*M*-*E*) under 80 Oe. All samples are sufficiently magnetized before making each *M*-*E* curve to ensure the same initial magnetic state, and the electric field changes as follows: 0 kV/cm, −12 kV/cm, 12 kV/cm, −12 kV/cm, and 0 kV/cm. Obviously, all the *M*-*E* curves are consistent with the butterfly like strain curve of PMN-PZT. The peaks in *M*-*E* and *S*-*E* curves, 4.1 kV/cm and 4.3 kV/cm, respectively, are close but not exactly the same. This is mainly due to the fact that the applied electric field in the case of *M*-*E* is DC, while in the other case, it is ac.[17] Nonetheless, we can confirm the efficiency of strain-mediated ME coupling in this ferrite-piezoelectric structure. The magnitude of magnetization corresponds to the data in *M*-*H* curves at 80 Oe [inset of Fig. 3(a)]. In addition, the peak depth (ΔM) marked in Fig. 4(a) increases with the increase in the film thickness at a given bias magnetic field. For the sake of comparison, we represent ΔM as a function of the bias magnetic field (80, 20, and 10 Oe) with respect to the film thickness, as shown in Fig. 4(b). It is noteworthy that the maximum ΔM for a certain thickness always appears at the coercive field of YIG (20 Oe) for the reason that the magnetic domains can be easily reversed here, and the thicker film has the potential to gain a larger magnetization shift. Figure 4(c) gives an example of the relationship between the *Mr* of the 200 nm-thick film and the external electric field. The variation cycle illustrated by the arrows implies an obvious change in the magnetic anisotropic field and so the efficient control of magnetization by the electric field. The CME coefficient (α) determined by the expression $\alpha = \mu_0 \delta M/\delta E$ ($\mu_0 = 4\pi \times 10^{-7}$ H/m)[3,17] is given in Fig. 4(d). The magnetic field for the maximum α in each α-*E* curve is near the peak position in the corresponding *M*-*E* curve, and the maximum α increases with the increasing thickness. The situation under 20 and 10 Oe is similar to the one observed under 80 Oe.

Analogously, the calculated maximum CME coefficient as a function of the bias magnetic field under different YIG thicknesses is presented in Fig. 5. Two similar phenomena to those already observed in the case of ΔM-*H* are noticed: (i) the maximum α appears at 20 Oe for all YIG thicknesses, which is probably ascribed to the easy magnetization switching at this point as all the *Hc* values are around it [inset of Fig. 3(a)] and the magnetic susceptibilities reach the maximum also around 20 Oe [Fig. 3(b)]; and (ii) the thicker film exhibits the stronger CME coupling due to the lower roughness, the better crystallization and magnetic properties, and maybe the less strain relaxation in the film. As a result, a remarkable CME coefficient of 3×10^{-7} s/m can be achieved on the sample with a 600 nm-thick YIG film at 20 Oe, which is 5-fold greater than the α value obtained for LSMO/PMN-PT(001)[17] but lower than CoFeB/PMN-PT (011).[20] The magnetostrictive and the piezo strain performances of the materials which compose the heterostructure have obviously a strong influence on the CME coefficient. A larger comparative study involving different kinds of multiferroic systems has been proposed recently.[21]

Finally, we extrapolate the α-*H* curves to predict the values at 0 Oe to see whether it is possible to get significant CME effects in this system with a magnetized YIG film in the absence of a bias magnetic field. The predicted results and the values at 20 Oe are listed in Table I. Representatively, the 600 nm-thick magnetized film would possess a CME coefficient of 2.2×10^{-7} s/m without an external magnetic field. These results not only demonstrate the validity of strain-mediated CME coupling in this ferrite-piezoelectric heterostructure but

TABLE I. The values of saturation magnetization (*Ms*), residual magnetization (*Mr*), coercive field (H_C), magnetic susceptibility (χ), and CME coefficient (α) at 20 and 0 Oe (predicted) of YIG films with different thicknesses.

t of YIG (nm)	*Ms* (emu/cm^3)	*Mr* (emu/cm^3)	*Hc* (Oe)	χ_{max} at 20 Oe	α at 20 Oe (10^{-7} s/m)	α at 0 Oe (10^{-7} s/m)
200	110.4	46.9	23.4	36.4	1.2	0.9
400	129.3	56.6	20.1	45.4	1.3	1.0
600	146.7	50.6	17.2	42.2	3.1	2.2

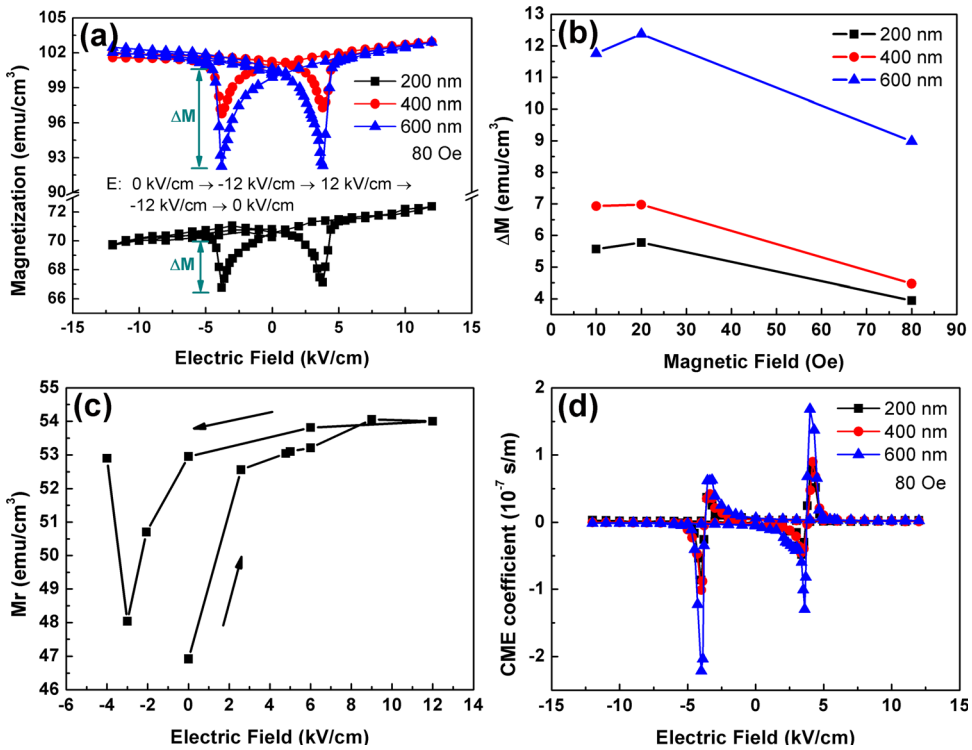

FIG. 4. The electric field dependencies of magnetization (a) under 80 Oe in the YIG films of different thicknesses. (b) ΔM (peak depth defined in (a)) in M-E curves as a function of the bias magnetic field. (c) The impact of the electric field on the Mr of the 200 nm-thick YIG film. The process is traced by the arrows. (d) The electric field dependencies of the CME coefficients calculated from (a).

also promote the realization of more compact and power efficient ME devices that can achieve a strong ME effect under a small electric field and a small or even zero magnetic field.

In summary, the converse magnetoelectric effect is investigated through the electric field tuning of magnetization based on the composite consisting of YIG films with different thicknesses and a 0.25PMN-0.75PZT ceramic. The experimental results show that every magnetization-electric field curve is in good agreement with the ceramic strain evolution. The enhancement of the CME interaction at the small electric coercive field of PMN-PZT (4.1 kV/cm) and the small magnetic coercive field of YIG (20 Oe) is attributed to the combined effect of the sharp deformation of about 2.5‰ of PMN-PZT and the easier magnetization change in YIG. A remarkable CME coefficient of 3.1×10^{-7} s/m is observed on the composite comprising a 600 nm-thick YIG. This heterostructure of YIG/PMN-PZT with partially magnetized YIG is promising to obtain a strong CME effect under a small electric field and a small or even in the absence of a magnetic field, which open the doors to compact and power efficient devices.

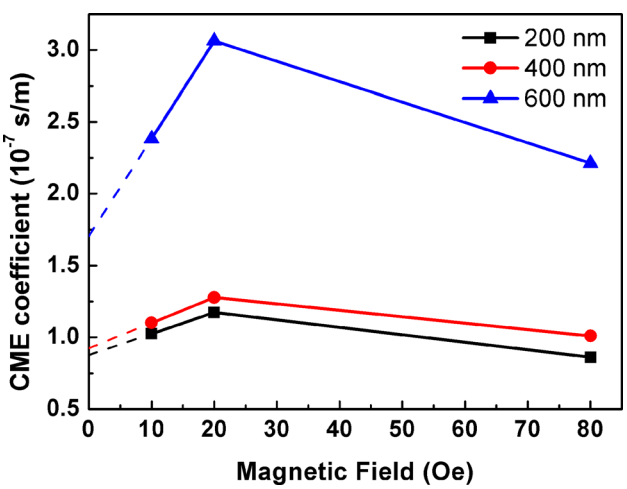

FIG. 5. The maximum CME coefficients in α-E curves as a function of the bias magnetic field for different film thicknesses. The extrapolated lines give a prediction of the situation under zero H.

This work was supported by the International Partnership Program of Chinese Academy of Sciences (Grant No. GJHZ1821) and the National Natural Science Foundation of China (U153010140) and funded by the Chinese Academy of Sciences President's International Fellowship Initiative (Grant No. 2017VEA0002).

[1]I. V. Zavislyak, M. A. Popov, G. Sreenivasulu, and G. Srinivasan, Appl. Phys. Lett. **102**, 222407 (2013).
[2]A. Klimov, N. Tiercelin, Y. Dusch, S. Giordano, T. Mathurin, P. Pernod, V. Preobrazhensky, A. Churbanov, and S. Nikitov, Appl. Phys. Lett. **110**, 222401 (2017).
[3]T. H. E. Lahtinen, K. J. A. Franke, and S. van Dijken, Sci. Rep. **2**, 258 (2012).
[4]M. I. Bichurin, I. A. Kornev, V. M. Petrov, A. S. Tatarenko, Y. V. Kiliba, and G. Srinivasan, Phys. Rev. B **64**, 094409 (2001).
[5]S. W. Yang, R. C. Peng, T. Jiang, Y. K. Liu, L. Feng, J. J. Wang, L. Q. Chen, X. G. Li, and C. W. Nan, Adv. Mater. **26**(41), 7091 (2014).
[6]Z. Y. Zhou, M. Trassin, Y. Gao, D. N. Qiu, K. Ashraf, T. X. Nan, X. Yang, S. R. Bowden, D. T. Pierce, M. D. Stiles, J. Unguris, M. Liu, B. M. Howe, G. J. Brown, S. Salahuddin, R. Ramesh, and N. X. Sun, Nat. Commun. **6**, 6082 (2015).
[7]M. Liu, Z. Zhou, T. Nan, B. M. Howe, G. J. Brown, and N. X. Sun, Adv. Mater. **25**, 1435 (2013).
[8]J. Lou, M. Liu, D. Reed, Y. Ren, and N. X. Sun, Adv. Mater. **21**(46), 4711 (2009).

[9]J. Das, Y. Y. Song, N. Mo, P. Krivosik, and C. E. Patton, Adv. Mater. **21**(20), 2045 (2009).
[10]J. H. Leach, J. Appl. Phys. **108**, 064106 (2010).
[11]Y. K. Fetisov and G. Srinivasan, Appl. Phys. Lett. **93**, 033508 (2008).
[12]A. B. Ustinov and G. Srinivasan, Tech. Phys. **55**(6), 900 (2010).
[13]S. Shastry, G. Srinivasan, M. I. Bichurin, V. M. Petrov, and A. S. Tatarenko, Phys. Rev. B **70**, 064416 (2004).
[14]A. B. Ustinov, G. Srinivasan, and Y. K. Fetisov, J. Appl. Phys. **103**, 063901 (2008).
[15]X. Yang, Y. Gao, J. Wu, Z. Zhou, S. Beguhn, T. Nan, and N. X. Sun, IEEE Microwave Wireless Compon. Lett. **24**(3), 191 (2014).
[16]L. Wang, R. H. Liang, C. L. Mao, G. Du, G. S. Wang, and X. L. Dong, Ceram. Int. **39**(7), 8571 (2013).
[17]C. Thiele, K. Dörr, O. Bilani, J. Rödel, and L. Schultz, Phys. Rev. B **75**, 054408 (2007).
[18]J. Y. Lian, Y. Chen, Z. Liu, M. K. Zhu, G. S. Wang, W. B. Zhang, and X. L. Dong, Ceram. Int. **43**(10), 7477 (2017).
[19]N. Tiercelin, A. Talbi, V. Preobrazhensky, P. Pernod, V. Mortet, K. Haenen, and A. Soltani, Appl. Phys. Lett. **93**, 162902 (2008).
[20]S. Zhang, Y. G. Zhao, X. Xiao, Y. Wu, S. Rizwan, L. Yang, P. Li, J. Wang, M. Zhu, H. Zhang, X. Jin, and X. Han, Sci. Rep. **4**, 3727 (2014).
[21]M. Staruch, D. B. Gopman, Y. L. Iunin, R. D. Shull, S. F. Cheng, K. Bussmann, and P. Finkel, Sci. Rep. **6**, 37429 (2016).